

Automatic Clinical Image Segmentation using Pathological Modelling, PCA and SVM

Shuo Li¹, Thomas Fevens¹, Adam Krzyzak¹, and Song Li²

¹ Medical Imaging Group,

Department of Computer Science and Software Engineering

Concordia University, Montréal, Québec, Canada

{shuo.li, fevens, krzyzak}@cs.concordia.ca

² School of Stomatology, Anhui Medical University, Hefei, Anhui, P. R. China

xlisong@sohu.com

Abstract. A general automatic method for clinical image segmentation is proposed. Tailored for the clinical environment, the proposed segmentation method consists of two stages: a learning stage and a clinical segmentation stage. During the learning stage, manually chosen representative images are segmented using a variational level set method driven by a pathologically modelled energy functional. Then a window-based feature extraction is applied to the segmented images. Principal component analysis (PCA) is applied to these extracted features and the results are used to train a support vector machine (SVM) classifier. During the clinical segmentation stage, the input clinical images are classified with the trained SVM. By the proposed method, we take the strengths of both machine learning and variational level set while limiting their weaknesses to achieve automatic and fast clinical segmentation. Both chest (thoracic) computed tomography (CT) scans (2D and 3D) and dental X-rays are used to test the proposed method. Promising results are demonstrated and analyzed. The proposed method can be used during preprocessing for automatic computer aided diagnosis.

Keywords: image segmentation, support vector machine, machine learning, principal component analysis, dental X-rays

1 Introduction

Image segmentation is an important component of medical imagery which plays a key role in computer assisted medical diagnosis. Segmentation of medical images is typically more challenging than the segmentation of images in other fields. This is primarily due to a large variability in topologies, the complexity of medical structures and poor image modalities such as noise, low contrast, several kinds of artifacts and restrictive scanning methods. This is especially true for volumetric medical images where a large amount of data is coupled with complicated 3D anatomical structures. This paper reports innovative work using machine learning techniques such as the support vector machine (SVM) and principal component analysis (PCA) learning with a pathologically modelled variational

level set method to address the most challenging problems in the medical image analysis: clinical image segmentation and analysis. Although the SVM has been used in image segmentation, it is usually used during an intermediate step [1–3]. This is the first such work which uses the SVM directly for medical image segmentation, to the best of our knowledge.

One of latest techniques in medical image segmentation is based on a class of deformable models, referred as “level set” or “geodesic active contours/surfaces.” The application of the level set method in medical image segmentation is extremely popular due to its ability to capture the topology of shapes in medical imagery. Codimension-two geodesic active contours were used in [4] for tubular structures. The fast marching algorithm [5] and level set method were used in [6] and [7], while Region competition, introduced in [8], was used in [9]. In [2, 3, 10], Li *et al.* applied a variational level set segmentation approach, accelerated by an SVM, for medical image segmentation, analysis and visualization.

Although efficient, level set methods are not suitable for general use clinical image segmentation due to several reasons: (1) high computational cost; (2) complicated parameter settings; (3) sensitivity to the placement of initial contours. With regard to the latter, as will be shown in experimental results, the running time of the level set method heavily relies on the position and size of initial curves and geometric and topological complexity of objects. Moreover for some cases, the coupled level set method does not converge for some initial curves.

To overcome the current challenges in clinical image segmentation, in this paper, we combine the level set method approach with a machine learning technique. We employ the level set method only during the training stage of the SVM which limits the effect of the weaknesses (i.e., the slowness and lack of stability) of the level set method. Through the application of PCA, we then use the SVM exclusively for segmentation which leads to faster and more robust segmentation.

2 Proposed Method

The proposed method consists of two stages: a learning stage and a clinical segmentation stage. During the segmentation stage, a variational level set method driven by a pathologically modelled energy functional is used. This is followed by window-based feature extraction using PCA analysis. The extracted features are used to train an SVM. During the clinical segmentation, the clinical image is directly segmented by the trained SVM.

2.1 Level Set Method

Proposed by Osher and J. Sethian [5], level set methods have attracted much attention from researchers from different areas. In problems of curve evolution, the level set method and in particular the motion by mean curvature of Osher and Sethian [5] have been used extensively. This is because these methods allow for

curve characteristics such as cusps, corners, and automatic topological changes. Moreover, the discretization of the problem is made on the regular grid.

Let Ω be a bounded open subset of R^2 , with $\partial\Omega$ as its boundary. Let $U_0: \Omega \rightarrow R$ be a given image, and $C: [0, 1] \rightarrow R^2$ be a parameterized curve. The curve C is represented implicitly via a Lipschitz function ϕ , where $C = \{(x, y) | \phi(x, y) = 0\}$, and the evolution of the curve is given by the zero-level curve at time t as the function $\phi(t, x, y)$. Evolving the curve C in normal direction with speed F leads to the differential equation

$$\begin{cases} \frac{\partial\phi}{\partial t} = |\nabla\phi|F \\ \phi(0, x, y) = \phi_0(x, y) \end{cases} \quad (1)$$

where the set $C = \{(x, y) | \phi_0(x, y) = 0\}$ defines the initial contour. A particular case is the motion by mean curvature, when $F = \text{div}(\frac{\nabla\phi}{|\nabla\phi|})$ is the curvature.

2.2 Variational Level Set Method

Chan *et al.* [11, 12] proposed an Mumford-Shah functional for level set segmentation. They add a minimal variance term E_{MV} . The model is able to detect contours both with or without a gradient. Objects with smooth boundaries or even with discontinuous boundaries can be successfully detected. Moreover they claim this model is robust to the position of initial the initial contour. The 2D version of the model can be expressed as

$$\inf_{(c_1, c_2, C)} E = \mu \cdot \text{Length}(C) + v \cdot \text{Area}(\text{Inside}(C)) + E_{MV}$$

with

$$E_{MV} = \lambda_1 \int_{\text{inside}(C)} |u_0(x, y) - c_1| dx dy + \lambda_2 \int_{\text{outside}(C)} |u_0(x, y) - c_2| dx dy$$

where c_i are the averages of u_0 inside and outside C , and $\mu \geq 0$, $v \geq 0$, $\lambda_1 > 0$ and $\lambda_2 > 0$ are fixed parameters.

The level set function they obtain is given by

$$\begin{cases} \frac{\partial\phi}{\partial t} = \delta_\varepsilon(\phi) [\mu \cdot \text{div}(\frac{\nabla\phi}{|\nabla\phi|}) - v - \lambda_1(u_0 - c_1)^2 + \lambda_2(u_0 - c_2)^2] = 0 \\ \phi(0, x, y) = \phi_0(x, y) \text{ in } \Omega \\ \frac{\delta_\varepsilon(\phi)\partial\phi}{|\nabla\phi|\partial\mathbf{n}} = 0 \text{ on } \partial\Omega. \end{cases}$$

where \mathbf{n} denotes the exterior to the boundary $\partial\Omega$, $\frac{\partial\phi}{\partial\mathbf{n}}$ denotes the normal derivative of ϕ at the boundary and δ_ε is the Dirac delta function.

The Chan and Vese functional is very good for segmenting an image into two regions. To segment images with multiple regions we use Samson's method. In [13], Samson *et al.* presented a variational approach as shown in Eqs. 2 and 3.

$$\begin{aligned} \inf E = & \sum_{1 \leq i \leq j \leq n} f_{ij} \text{Length}(\Gamma_{ij}) + \sum_{1 \leq i \leq n} v_i \text{Area}(\text{Inside}(C_i)) \\ & + \sum_i \int_{\Omega_i} e_i \frac{(u_0 - c_i)^2}{\sigma_i^2} dx dy + \frac{\lambda}{2} \int (\sum_{j=1}^n H(\phi_j) - 1)^2 dx dy. \end{aligned} \quad (2)$$

where Γ_{ij} is the intersection of different regions and σ_i is the variance. The level set function they obtain is given by

$$\begin{cases} \frac{\partial \phi_i}{\partial t} = \delta_\varepsilon(\phi_i) \left(\gamma_i \operatorname{div} \left(\frac{\nabla \phi}{|\nabla \phi|} \right) - e_i \frac{(u_0 - c_i)^2}{\sigma_i^2} - \lambda \left(\sum_{j=1}^n H(\phi_j) - 1 \right) \right) \\ \frac{\partial \phi_i}{\partial n} = 0 \text{ on } \partial \Omega. \end{cases} \quad (3)$$

where $H(\cdot)$ is the Heaviside function.

2.3 Pathologically Modelled Variational Level Set Method

In this work, we apply the variational level set method to segment the representative images. First, with the assistance of a doctor or clinician, the energy functional will be modelled according to the pathological meaning of different regions in an image. In the following we are going to take chest CT (2D and 3D) scans and dental X-ray images as examples as can be seen in Fig. 1.

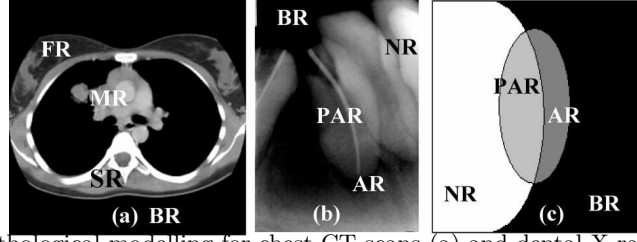


Fig. 1. Pathological modelling for chest CT scans (a) and dental X-rays (b and c).

Chest CT Scan Fig. 1(a) demonstrates a pathological modelling for chest (thoracic) computed tomography (CT) scans. The images can be divided into four regions of interest: the Background Region (Ω_{BR}), the Skeletal Structure (bone) Region (Ω_{SR}), the Fatty Tissue Region (Ω_{FR}) and the Muscle and Visceral Tissue Region (Ω_{MR}). Energy functional for the four coupled level set functions are modelled as Eq. 4.

$$\begin{aligned} E_{MV}(\phi_i) = & \int_{\Omega_{BR}} \frac{e_1(u - c_{BR})^2}{\sigma_{NR}^2} dx dy + \int_{\Omega_{FR}} \frac{e_2(u - c_{FR})^2}{\sigma_{FR}^2} dx dy + \\ & \int_{\Omega_{SR}} \frac{e_3(u - c_{SR})^2}{\sigma_{SR}^2} dx dy + \int_{\Omega_{MR}} \frac{e_4(u - c_{MR})^2}{\sigma_{MR}^2} dx dy \end{aligned} \quad (4)$$

where $c_i, i=1, \dots, 4$, is the mean grey value of region Ω_i .

Dental X-ray With prior information, this pathological modelling can also be used for computer aided diagnosis. As shown in the Figs. 1 (b) and (c), X-ray images can be divided into four regions of interest: the Normal Region (Ω_{NR}), the Potentially Abnormal Region (Ω_{PAR}), the Abnormal Region (Ω_{AR}) and the Background Region (Ω_{BR}). Since Ω_{AR} and Ω_{BR} are not separable in terms

of intensity values, so in the segmentation, we take Ω_{AR} and Ω_{BR} to be one region: the Abnormal and Background Region (Ω_{ABR}). Energy functional for three coupled level set functions are modelled as Eq. 5.

$$E_{MV}(\phi_i) = e_1 \int_{\Omega_{NR}} \frac{(u - c_{NR})^2}{\sigma_{NR}^2} dx dy + e_2 \int_{\Omega_{PAR}} \frac{(u - c_{PAR})^2}{\sigma_{PAR}^2} dx dy + e_3 \int_{\Omega_{ABR}} \frac{(u - c_{ABR})^2}{\sigma_{ABR}^2} dx dy. \quad (5)$$

The proposed pathological modelling explicitly incorporates regions of problems as part of the modelling, the identification of such areas would be an automatic byproduct of the segmentation. Moreover those problem regions generally indicate some possible areas of bone loss in teeth or the jaw or root decay, which are the primary reasons that X-rays are taken in many countries. Early detection of bone loss and root decay is very important since often they can be remedied by dental procedures, such as a root canal, for example. Without early treatment, bone loss may lead to tooth loss or erosion of the jaw bone.

2.4 Learning

As shown in Fig. 2, the learning phase consists of several steps. First, manually chosen images are segmented by the variational level set described in section 2.3. To avoid distraction, the high uncertainty areas are removed. Next, window-based feature extraction is applied. The results will be used to train the SVM after applying PCA learning to extract features.

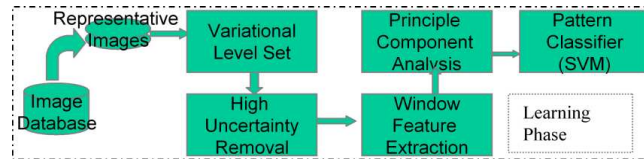


Fig. 2. Learning phase diagram.

Uncertainty Removal Before feature extraction, those areas of high uncertainty in the segmented image will be removed to avoid the possible distraction. The uncertainty measurement is the product of two components: a numerical solution uncertainty component $\psi_1(x, y)$ and a variance uncertainty component $\psi_2(x, y)$ as shown:

$$\psi(x, y) = \psi_1(x, y) \cdot \psi_2(x, y) = \frac{1 + \max(H(\phi_i))}{1 + \sum H(\phi_i)} \cdot \frac{\sum \sigma_i H(\phi_i)}{\sum |u - c_i| H(\phi_i)}$$

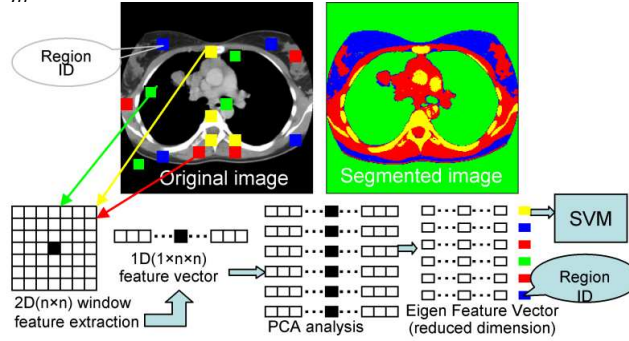


Fig. 3. Feature extraction diagram

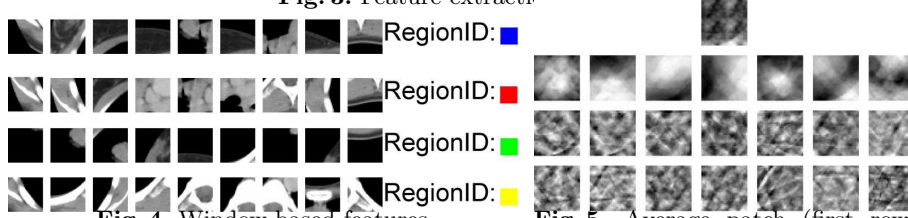


Fig. 4. Window based features.

Fig. 5. Average patch (first row) and eigen patches.

Feature extraction and principal component analysis A window-based feature extraction is applied to each segmented region in the image. This is illustrated in Fig. 4. The PCA method used here is adapted from [14, 15]. Let the features Γ_i ($i = 1..M$) constitute the training set (Γ). The average matrix ($\bar{\Gamma}$) and covariance matrix C are:

$$\begin{aligned}
 \bar{\Gamma} &= \frac{1}{M} \sum_{i=1}^M \Gamma_i \\
 \Phi_i &= \Gamma_i - \bar{\Gamma} \\
 C &= \frac{1}{M} \sum_{i=1}^M \Phi_i^T \Phi_i = AA^T \\
 L &= A^T A (L_{n,m} = \Phi_n^T \Phi_m) \\
 u_i &= \sum_{k=1}^M v_{ik} \Phi_k (l = 1, \dots, M)
 \end{aligned} \tag{6}$$

where L is a $M \times M$ matrix, v_{ik} are the M eigenvectors of L and u_i are eigen-patches which was called eigenfaces in [14, 15]. The advantage of the PCA analysis here is its ability to remove the effects of noise and also to accelerate the classification by reduced feature dimension.

SVM Training and Segmentation The strength of the SVM classifier has been demonstrated in many research areas such as handwriting recognition application, which is described in Dong *et al.* [16, 17]. The classifier we use is a modified version of the SVM classifier proposed in [18].

3 Results

To evaluate the proposed method, both chest CT scans (two dimensional and three dimensional images) and dental X-ray images are used to test the proposed method.

3.1 Chest CT Scans

Two Dimensional Scans Figs. 6 and 7 show the results of two dimensional image segmentation. Fig. 6 shows the results of pathological variational level set segmentation which divides the image into four regions of background, the skeletal structure (bone), the fatty tissue, and the muscle and visceral tissue, as defined in section 2.3. However the variational level set method is a time consuming method which generally takes longer than 10 minutes to segment a 256×256 image for a PC (Pentium 1G Hz and 1GRAM). Moreover, for some cases, level set methods, especially for coupled level set methods, may not converge for some initial curves as pointed out in [3, 19, 20] which limit the usage of the level set method in clinical image processing which has high requirements on speed and robustness. Fig. 7 demonstrates the segmentation results using the proposed method which just takes around 1 second.

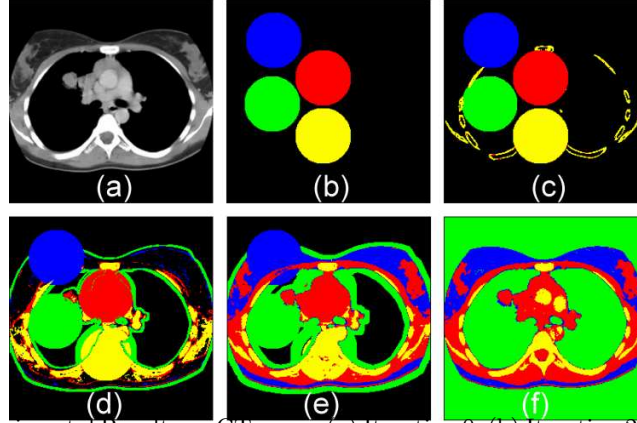


Fig. 6. Experimental Results on CT scans. (a) Iteration 0. (b) Iteration 20. (c) Iteration 50. (d) Iteration 100.

Three Dimensional Scans Figs. 8 and 9 show results on three dimensional image segmentation. Fig. 8 shows variational level set segmentation on volumetric CT scan image ($256 \times 256 \times 100$) which usually takes longer than 2 hours while with our proposed method takes around 20 seconds.

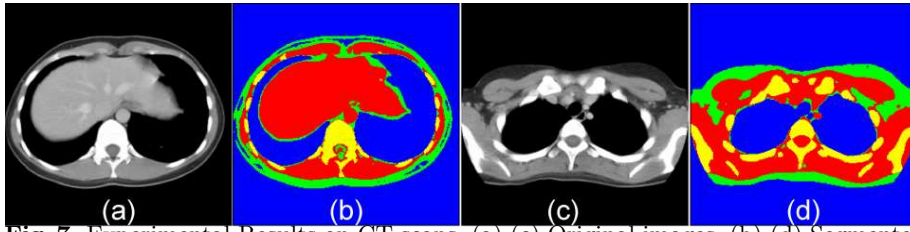


Fig. 7. Experimental Results on CT scans. (a) (c) Original images. (b) (d) Segmented images.

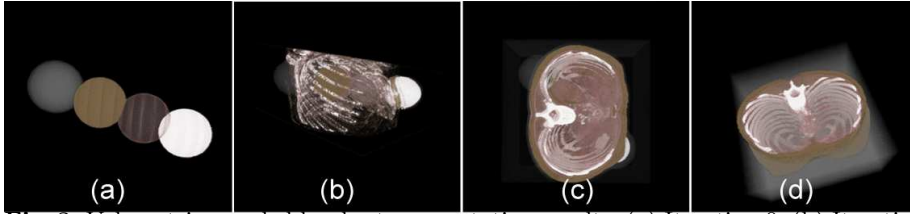


Fig. 8. Volumetric coupled level set segmentation results. (a) Iteration 0. (b) Iteration 30. (c) Iteration 80. (d) Iteration 120.

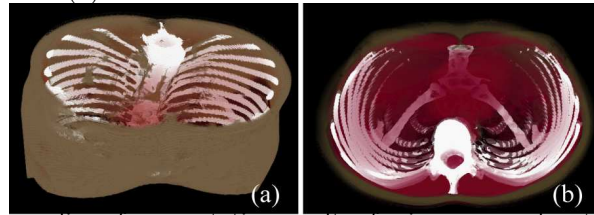


Fig. 9. Volume rendering of segmentation results of using proposed method on chest CT scans. (a) One View. (b) Another view.

3.2 Dental X-ray Images

Dental X-ray segmentation is a challenging problem for classic methods due to the following characteristics: (1) poor image modalities: noise, low contrast, and sample artifacts; (2) complicated topology; and (3) there may not be clear edges between regions of interest which is especially true for dental images with early stage problem teeth. Fig. 10 demonstrates the variational level set segmentation described in section 2.3 on dental X-ray images. As can be seen, the variational level set method is able to successfully segment with the given pathological modelling which provides automatic feature extraction for PCA and SVM training. Fig. 11 shows the results by the proposed method. Since pathological modelling explicitly incorporates regions of problems as part of the modelling, the identification of such areas is an automatic byproduct of the segmentation.

4 Conclusion

This paper proposes a general automatic clinical image segmentation method. The proposed segmentation method contains two stages: a learning stage and a clinical segmentation stage. During the learning stage, manually chosen representative images are segmented using a variational level set method driven

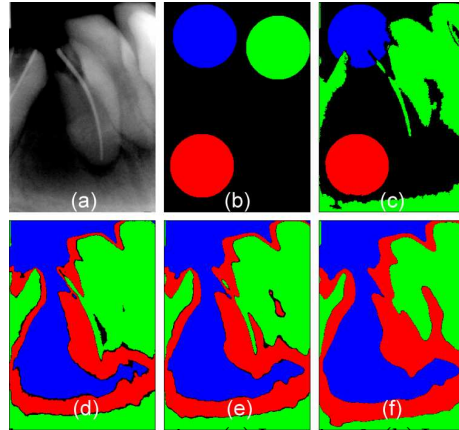


Fig. 10. Coupled level sets segmentation. (a) Iteration 0. (b) Iteration 100. (c) Iteration 500. (d) Iteration 1000. (e) Iteration 1500. (f) Iteration 2000.

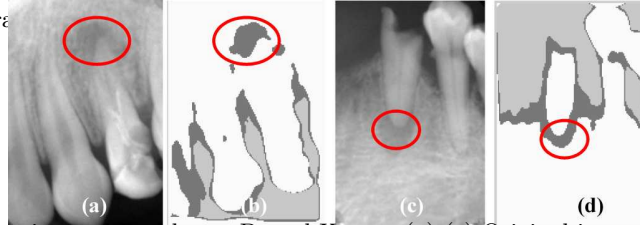


Fig. 11. Experimental Results on Dental X-rays. (a) (c) Original image with problem area circled by dentist. (b) (d) Segmented image.

by a pathologically modelled energy functional. Then a window-based feature is extracted from the segmented images and the principal component analysis is applied to those extracted features. These results are used to train a support vector machine classifier. During the segmentation stage, the clinical images are classified with the trained SVM. The proposed method takes the strengths of newly developed machine learning and the variational level set methods while limiting their weaknesses to achieve a automatic and fast clinical segmentation. The method is tested with both chest CT scans and dental X-ray images. These results show that the proposed method is able to provide a fast and robust clinical image segmentation of both 2D and 3D images. Due to the use of pathological modelling to define the regions of interest, the segmentation results can be used to further analyze the image. The proposed method can be used as pre-processing step for automatic computer aided diagnosis. We are currently studying other machine learning algorithms for the analysis of segmented images to provide further improved assistance to the doctor or clinician.

References

1. S. Wang, W. Zhu, and Z.-P. Liang, "Shape deformation: SVM regression and application to medical image segmentation," in *ICCV*, pp. 209–216, 2001.
2. S. Li, T. Fevens, and A. Krzyżak, "An SVM based framework for autonomous volumetric medical image segmentation using hierarchical and coupled level sets," in *Computer Aided Radiology and Surgery (CARS)*, (Chicago, USA), pp. 207–212, 2004.

3. S. Li, T. Fevens, and A. Krzyżak, “Image segmentation adapted for clinical settings by combining pattern classification and level sets,” in *Medical Image Computing and Computer-Assisted Intervention (MICCAI)*, (St-Malo, France), pp. 160–167, 2004.
4. L. M. Lorigo, W. E. L. Grimson, O. D. Faugeras, R. Keriven, R. Kikinis, A. Nabavi, and C.-F. Westin, “Codimension-two geodesic active contours for the segmentation of tubular structures,” in *IEEE Conf. Computer Vision and Pattern Recognition*, 2000.
5. S. Osher and J. A. Sethian, “Fronts propagating with curvature-dependent speed: Algorithms based on Hamilton-Jacobi formulations,” *Journal of Computational Physics*, vol. 79, pp. 12–49, 1988.
6. R. Kimmel and A. M. Bruckstein, “Regularized Laplacian zero crossings as optimal edge integrators,” *International Journal of Computer Vision*, vol. 53, pp. 225–243, July 2003.
7. A. Vasilevskiy and K. Siddiqi, “Flux maximizing geometric flow,” *IEEE Trans. on Pattern Analysis and Machine Intelligence*, vol. 24, no. 12, pp. 1565–1578, 2002.
8. S. Zhu and A. Yuille, “Region competition: Unifying snakes, region growing, energy/bayes/mdl for multiband image segmentation,” *IEEE Trans. on Pattern Analysis and Machine Intelligence*, vol. 19(9), pp. 884–900, 1996.
9. V. Caselles, F. Catte, T. Coll, and F. Dibos, “A geometric model for active contours,” *Numer. Math.*, vol. 66, pp. 1–31, 1993.
10. S. Li, T. Fevens, A. Krzyżak, and S. Li, “Level set segmentation for computer aided dental X-ray analysis,” in *SPIE Conference on Medical Imaging*, (San Diego, USA), 2005. Accepted.
11. T. Chan and L. Vese, “Active contour model without edges,” *IEEE Trans. on Image Processing*, vol. 24, pp. 266–277, 2001.
12. L. Vese and T. Chan, “A multiphase level set framework for image segmentation using the mumford and shah model,” *International Journal of Computer Vision*, vol. 50, no. 3, pp. 271–293, 2002.
13. C. Samson, L. Blanc-Fraud, G. Aubert, and J. Zerubia, “A level set model for image classification,” *International Journal of Computer Vision*, vol. 40, no. 3, pp. 187–197, 2000.
14. M. Turk and A. Pentland, “Face recognition using eigenfaces,” in *Proc. IEEE Conference on Computer Vision and Pattern Recognition*, (Hawaii), 1991.
15. M. Turk and A. Pentland, “Eigenfaces for recognition,” *Journal of Cognitive Neuroscience*, vol. 3, no. 1, pp. 71–86, 1991.
16. J. Dong, A. Krzyżak, and C. Y. Suen, “A fast parallel optimization for training support vector,” in *International Conference on Machine Learning and Data Mining (MLDM)* (P. Perner and A. Rosenfeld, eds.), vol. LNAI 2734, (Leipzig, Germany), pp. 96–105, Springer Lecture Notes in Artificial Intelligence, July 2003.
17. J. Dong, A. Krzyżak, and C. Y. Suen, “Fast SVM training algorithm with decomposition on very large training sets,” *IEEE Trans. on Pattern Analysis and Machine Intelligence*, 2005. to appear.
18. C.-C. Chang and C.-J. Lin, “Training nu-support vector classifiers: theory and algorithms,” *Neural Computation*, vol. 13, no. 9, pp. 2119–2147, 2001.
19. M. Holtzman-Gazit, D. Goldsher, and R. Kimmel, “Hierarchical segmentation of thin structure in volumetric medical images,” in *Medical Image Computing and Computer-Assisted Intervention (MICCAI)*, (Montreal), 2003.
20. A. Tsai, A. Yezzi, and A. S. Willsky, “Curve evolution implementation of the mumford-shah functional for image segmentation, denoising, interpolation, and magnification,” *IEEE Trans. on Image Processing*, vol. 10, pp. 1169–1186, 2001.